

# Intermodulation Interference Detection in 6G Networks: A Machine Learning Approach

Faris B. Mismar

Nokia Bell Labs Consulting, Murray Hill, NJ, 07974

**Abstract**—This paper demonstrates the use of machine learning to detect the presence of intermodulation interference across several wireless carriers. We show a salient characteristic of intermodulation interference and propose a machine learning based algorithm that detects the presence of intermodulation interference through the use of supervised learning. This algorithm can use the radio access network intelligent controller or the sixth generation of wireless communication (6G) edge node as a means of computation. Our proposed algorithm runs in linear time in the number of resource blocks, making it a suitable radio resource management application in 6G.

**Index Terms**—intermodulation, interference, detection, real-time, machine learning, 5G, 6G, edge computing.

## I. INTRODUCTION

As more frequency bands are introduced to the fifth generation of wireless networks (5G) and beyond (B5G), the combinations of the carriers used on the base stations increase. Combined with sources of intermodulation interference, which can be difficult to spot in the coverage area of a cell, the detection of intermodulation interference becomes ever important. The mitigation of intermodulation interference can help wireless operators improve the performance of the cell.

Intermodulation interference can be either active or passive based on the existence of active elements in the radio circuit. Active intermodulation interference can be avoided by not driving the amplifiers past their linear region. What remains is the passive intermodulation interference. Passive intermodulation can happen when deploying multiple frequency bands on a single network element (e.g., an antenna) to save physical space. Sources of passive intermodulation interference are either *internal* such as corroded junctions, duplexers, or cables that are contaminated with metallic particles, or *external* such as rusty bolts or fences. We will use the term *intermodulation interference* to refer to the passive type in this paper.

With the development of wireless communications systems beyond 5G, network and computing convergence platforms in the radio access network (RAN) such as the sixth generation of wireless communication (6G) “multi-access edge computing” are expected to be one of the enablers for machine learning applications that can operate in near real-time. Another example of these enablers is also present in the Open-RAN standards such as the RAN intelligent controller [1]. While the topic of intermodulation interference detection is not new, it is the use of machine learning based algorithms that can detect intermodulation near real-time and without test signals or noise simulators that makes this topic not only suitable for present

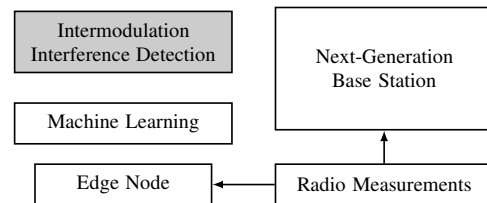


Fig. 1. Next-generation base station using machine learning in an edge node on radio measurements to detect the existence of intermodulation interference.

5G, but also—and through the use of edge computing—suitable for successive network evolutions.

Prior work related to detection of intermodulation interference was studied in [2]. A signal modeling method was proposed using block computations methods on third-order intermodulation products. This effectively has two limitations: 1) it focuses only on detection of third-order intermodulation products and 2) its processing delay per computational step is dependent on the sample (or the “block”) size. Our proposed method is not limited to third-order intermodulation products and has linear run-time complexity. In [3], the use of anomaly detection as a technique to detect performance abnormalities such as excessive uplink power was proposed. However, while the excessive uplink power anomaly could be a sign of intermodulation interference in the uplink frequency band, it could also be due to other impairments not related to intermodulation interference such as narrow-band interference. Industry standards such as [4] propose solutions that generate channel noise as a means to detect intermodulation interference. However, this brings *further* load and interference to a BS already suffering from impairments.

In this paper, we provide an answer to whether a reliable non-surgical method for intermodulation interference detection can be derived.

This paper makes two specific contributions:

- 1) Motivate why the intermodulation interference power spectral density in the presence of Fast Fourier Transform (FFT) is sloped and thus can be approximated by a line.
- 2) Use a machine learning algorithm based on simple linear regression that can detect intermodulation interference in real-time and *without* any surgical activities (e.g., injection of test tones or channel noise simulators).

## II. SYSTEM MODEL

We consider a system composed of a single base station (BS) with multiple transmit (i.e., downlink) and receive (i.e.,

uplink) frequencies each of a bandwidth  $B$ . Intermodulation interference sources and user equipment devices (UEs) are independently scattered in the service area of the BS. The system uses frequency division duplex (FDD) mode of operation, even though time division duplex (TDD) is also possible jointly with an FDD deployment or when different uplink-downlink frame configurations are elected for different frequency bands.

The system uses orthogonal frequency division multiplexing (OFDM) in both uplink and downlink\*. For simplicity of notation in the representation of the OFDM waveform in the time domain, we choose the  $k$ -th OFDM subcarrier at the time instant  $n$  using quadrature amplitude modulation and center frequency  $f_c$  and write:

$$x_{c,k}[n] = \text{Re} \left( g_B(t - nT) A_{c,k} e^{j2\pi k \Delta f (t - nT)} e^{j2\pi f_c t} \right) \quad (1)$$

where  $A_{c,k}$  is a complex signal of the inphase and quadrature components,  $\Delta f$  is the OFDM subcarrier spacing,  $T$  is the subcarrier duration, and  $g_B(t)$  is a *windowed* sinc pulse shaping function with bandwidth  $B$ . There are  $N_{\text{SC}}$  subcarriers in one physical resource block (PRB). The number of subcarriers  $N_{\text{SC}} = \lfloor B/\Delta f \rfloor$ . A PRB is the smallest non-overlapping frequency resource allocated in the fourth generation of wireless communication and its present evolutions [5]. The number of PRBs available for allocation ( $N_{\text{PRB}} > 0$ ) depends on the bandwidth  $B$ .

To potentially have intermodulation interference on the uplink or receive frequency band  $B'$ , at least two subcarriers (one from each transmit frequency) have to be combined at a non-linearity (e.g., intermodulation interference sources) such that their product falls in band with the uplink frequency band. We represent this non-linearity as an  $m$ -th order polynomial  $q: x \mapsto \sum_{k=1}^m a_k x^k$ , with  $a_k \neq 0$ .

### III. INTERMODULATION INTERFERENCE

Intermodulation interference may happen in any direction (i.e., uplink or downlink). However, it is particularly interesting in the uplink since UEs are power-limited (i.e., compared to BSs). This can make the uplink target signal-to-interference-plus-noise ratio more difficult to achieve causing access blockage and increased bit error rate. Intermodulation interference can happen due to two or multiple center frequencies and can be of any order  $m \geq 2$ .

For simplicity of math, we study the intermodulation interference due to two center frequencies, each being a subcarrier belonging to a distinct PRB, and up to the *third* intermodulation interference order. Let these two frequencies be  $f_1$  and  $f_2$  and the subcarriers  $x_{1,k}$  and  $x_{2,\ell}$  as follows from (1). Let us call the BS the transmit frequencies of which cause the intermodulation interference an ‘‘offender.’’

**Non-linearity:** When non-linearity is introduced between the voltage and current components of a signal, harmonic

\*We use OFDM as an umbrella term that may include proposed 6G variants (e.g., the Discrete Fourier Transform spread OFDM waveform in 5G).

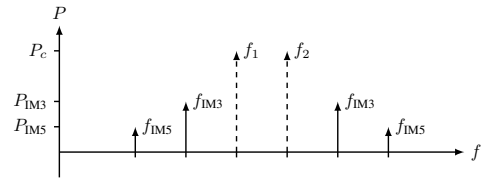


Fig. 2. OFDM tones (dashed) and their respective odd-order intermodulation products (solid).

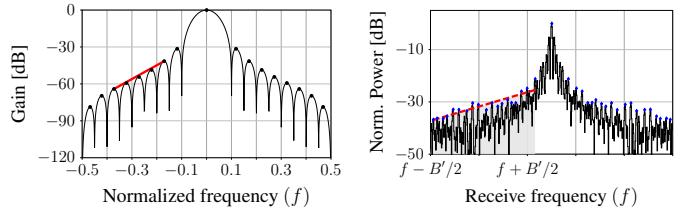


Fig. 3. Windowing spectral plots: (a) gain vs frequency plot of a window function (black) showing the side lobes (dotted peaks) and a line (red) the slope of which is equal to the rolloff rate (b) spectral leakage impact on intermodulation interference (black) in a receive frequency band  $B'$  (shaded) with side lobe peaks (blue dots) and a fitted line (dashed red) of the windowed intermodulation products.

frequencies and linear combinations of them are generated. For our signals  $x_{1,k}[n]$  and  $x_{2,\ell}[n]$ , we consider an input signal

$$x_{(k,\ell)}[n] = x_{1,k}[n] + x_{2,\ell}[n]. \quad (2)$$

This input signal, when passing through a non-linearity with  $m = 3$  creates an output signal  $y_{(k,\ell)}[n] := q(x_{(k,\ell)}[n])$ :

$$\begin{aligned} y_{(k,\ell)} &:= q(x_{1,k} + x_{2,\ell}) \\ &= a_1(x_{1,k} + x_{2,\ell}) + a_2(x_{1,k} + x_{2,\ell})^2 \\ &\quad + a_3(x_{1,k} + x_{2,\ell})^3. \end{aligned} \quad (3)$$

It is straightforward to substitute  $x_{1,k}$  and  $x_{2,\ell}$  in all the terms above with their respective OFDM waveform representation in (1). Examining the terms of  $y_{(k,\ell)}$ , there are first-order (or linear) terms which contain the *fundamental* center frequencies  $f_1$  and  $f_2$ . However, it is the quadratic and cubic terms that are of particular interest. Expanding these higher-order terms and using trigonometric identities, we obtain OFDM subcarriers at the following center frequencies:  $\{f_1, f_2, 2f_1, 2f_2, f_1 \pm f_2, 3f_1, 3f_2, 2f_1 \pm f_2, 2f_2 \pm f_1\}$ . Excluding the fundamental frequencies, we are left with second- and third-order harmonics. These could interfere with other receive bands in the vicinity.

**Intermodulation order:** The sum of the absolute values of the frequency multipliers define the intermodulation order. So, in the case of  $\{2f_1 \pm f_2, 2f_2 \pm f_1\}$ , we have third-order intermodulation products ( $f_{\text{IM}3}$ ). Let us call the portion of the output signal that has these third-order products  $y_{\text{IM}3}$ . A similar computation can be made for a fifth-order non-linearity. These are  $\{3f_1 \pm 2f_2, 3f_2 \pm 2f_1\}$  and are the fifth-order intermodulation products ( $f_{\text{IM}5}$ ). Similarly, the portion of the output signal that has those fifth-order products is  $y_{\text{IM}5}$ . Fig. 2 shows the third- and fifth-order intermodulation subtractive

products. These are the combinations (or “products”) involving a frequency difference and thus typically fall in-band of the receive PRBs. The third- and fifth-order products have a bandwidth of  $3B$  and  $5B$ .

**Intermodulation and duplex mode:** In FDD, the duplex gap (i.e., the difference between the downlink and uplink frequencies) dictates whether the subtractive products fall in the uplink frequency band. However, in TDD, the transmit and receive frequency bands are the same. Despite that, an odd-order intermodulation product (subtractive or additive) can fall in-band another TDD (or even FDD) receive frequency. In fact, with several frequency bands allocated for transmission and reception spanning sub-6 GHz waves, millimeter waves, and terahertz waves, it is possible for either even-ordered or additive intermodulation products (e.g.,  $f_1 + f_2$  or  $2f_1 + 2f_2$ ) to fall in-band one or more receive PRBs regardless of the duplex mode.

**Intermodulation characteristics:** We study the bandwidth, amplitude, and frequency difference between the intermodulation product and the fundamental frequency. Let us start with a relaxed version of the signal (1) where we set  $A_{c,k} = 1$  and compute the magnitude of the analytic part of the Fourier transform of  $x_{c,k}$  denoted as  $X_{c,k}(f)$ :

$$|X_{c,k}(f)| = \frac{1}{|\tilde{B}|} \left[ \text{rect} \left( \frac{f - f_c - k\Delta f}{B} \right) \right], \quad (4)$$

which is a rectangular pulse, with a base length (or *support*) of  $B$ . Here,  $\tilde{B} > 1$  is a collective term of coefficients. For the second-order intermodulation product ( $p = 2$ ) in  $y_{k,\ell}[t]$ , this product in the time domain is a convolution between two  $\text{rect}(\cdot)$  functions in the frequency domain. From this we make the following three observations:

- 1) Since each function has a support of  $B$ , their convolution  $Y_{k,\ell}(f)$  is a triangle function with a support (or *bandwidth*) of  $2B$ . The convolution of this triangle with another  $\text{rect}(\cdot)$  for the third-order product creates a function with a support of  $3B$ .
- 2) The amplitude of the convolved signal reduces as  $p$  increases. We find that the transmit power of the OFDM subcarrier  $P_1 = 1/(T|\tilde{B}|^2)$ . For the case of  $p = 2$ , we compute the power of the second-order intermodulation product as  $P_2 \simeq 1/(T|\tilde{B}|^3)$ , which is smaller than  $P_1$ .
- 3) The frequency difference of the intermodulation product center frequency to the fundamental center frequencies increase as  $p$  increases. For the case of  $p = 3$ , the difference between  $f_{\text{IM}3} = 2f_1 - f_2$  and the fundamental frequency  $f_1$  is  $f_1 - f_2$ . However, for  $p = 5$ ,  $f_{\text{IM}5} = 3f_1 - 2f_2$  this difference from  $f_1$  becomes  $2(f_1 - f_2)$ .

From these three findings, it follows that depending on the intermodulation product order  $p$ , the bandwidth  $B$ , and the fundamental frequencies, the intermodulation products can add up and fill up to a bandwidth of  $pB$ . In OFDM-based systems, where FFT is used for modulation, frequency content due to a windowing pulse-shaping function brings forward the concept of “spectral leakage.” [6]. Windowing and spectral leakage are shown in Fig. 3 where interference is spread across the

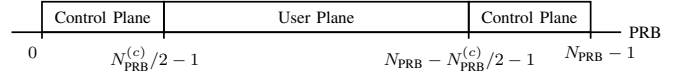


Fig. 4. Allocation of the control- and user-plane channels to the uplink PRBs.

entire band due to the frequency-domain convolution of the received signal with this windowing function at demodulation. This happens when a non-integer number of signal periods is sent to the FFT. System designs account for this constraint, which leaves interference as a cause of this leakage. Due to this and the three findings, the ability to detect the presence of intermodulation interference in such systems becomes as simple as detecting a sloped line in the power spectral density.

**Interference measures:** If we let  $P_c$  be the received power that correspond to one of the two fundamental frequencies in (3) and let the white Gaussian noise power spectral density be equal to  $N_0$  W/Hz, then we can write the received total power (RTP) in a given bandwidth as:

$$\text{RTP} := P_c + N_0B + P_I + \frac{1}{T} \sum_{p=2}^m \int_{pB} |Y_{\text{IM}p}(f)|^2 df, \quad (5)$$

where  $P_I$  is a term representing interference not due to intermodulation,  $P_{\text{IM}p}$  is the in-band  $p$ -th order intermodulation product interference power, and  $Y_{\text{IM}p}$  is the Fourier transform of  $y_{\text{IM}p}$ , which was defined for a given  $p$  earlier in this section. In the case of multi-input multi-output (MIMO) systems, RTP is computed per MIMO receive branch. These receive branches are independent and have separate hardware. The relationship between  $P_c$  and  $P_{\text{TX}}$  is governed by the path loss as we show here later. Also, if we let  $Y_{\text{IM}p}^{(\mathcal{P})}(f)$  be the output signal computed over the OFDM subcarriers in the PRB  $\mathcal{P} := \{\mathcal{P}_i\}_{i=0}^{N_{\text{PRB}}-1}$ , then with a little notation abuse we can write the RTP (5) for the  $j$ -th received branch as:

$$\text{RTP}_j := P_{c,j} + N_0B + P_{I,j} + \frac{1}{T} \sum_{i=0}^{N_{\text{PRB}}-1} \sum_{p=1}^m \int_{pB} |Y_{\text{IM}p,j}^{(\mathcal{P}_i)}(f)|^2 df. \quad (6)$$

**Internal or external:** Receive branches of a given antenna typically have identical hardware configuration and hence report similar RTP values. However, if RTP values differ and intermodulation interference is detected, then this can be due to an *internal* source of intermodulation interference. Also, if intermodulation interference is detected but the RTP values per receive branch are similar, then the source can be *external*.

It also follows from (6) that one way to mitigate intermodulation interference is to reduce the transmitted OFDM tone power of the *offender*, which is directly related to the BS transmit power ( $P_c := P_{\text{TX}} - L = P_{\text{BS}} - 10 \log N_{\text{PRB}} - 10 \log N_{\text{SC}} - L$ ), where  $P_{\text{BS}}$  is the BS transmit power in dBm and  $L$  is the path loss [7]. This power reduction also reduces the BS coverage radius.

At this stage in the development, it is important to mention that the standards also allocate certain PRBs for control-plane channels, while others are used for the user-plane channels.

Control channels are allocated the PRBs at the edges of the bandwidth. Let there be  $N_{\text{PRB}}^{(c)}$  PRBs allocated for control-plane channel and  $N_{\text{PRB}}^{(u)}$  allocated for the user-plane channel such that  $N_{\text{PRB}}^{(c)} + N_{\text{PRB}}^{(u)} = N_{\text{PRB}}$ , an example of which is shown in Fig. 4. Hence  $\mathcal{P} = \mathcal{P}^{(c)} \cup \mathcal{P}^{(u)}$ , written as a union of the sets of control- and user-plane PRBs.

An important quantity is the received interference power (RIP), which is measured in Watts per PRB—as defined in [8]—since PRBs are the smallest frequency resource allocated. For the  $r$ -th PRB where  $r \in \{0, 1, \dots, N_{\text{PRB}} - 1\}$ , we write:

$$\begin{aligned} \text{RIP}(r) := & \sum_{p=1}^m \int_{pB^{(r)}} N_0 \text{rect} \left( \frac{f - f_{\text{IM}p}}{pB^{(r)}} \right) df + P_I^{(r)} + \\ & \frac{1}{T} \sum_{p=2}^m \int_{pB^{(r)}} |Y_{\text{IM}p}(f)|^2 df, \end{aligned} \quad (7)$$

where  $B^{(r)}$  is the bandwidth of the  $r$ -th PRB in  $\mathcal{P}$  and  $P_I^{(r)}$  is a term representing interference not due to intermodulation as measured by the  $r$ -th PRB. Plotting the RIP against the PRBs in  $\mathcal{P}$  is a plot of noise plus interference power vs frequency and is therefore a power spectral density plot.

Owed to the selection of a windowing function and its side lobe rolloff rate [9], the power spectral density of spectral leakage (in dBm units) in the presence of interference can be approximated as a sloped line with a slope equal to the rolloff rate. Otherwise, RIP—as in (7)—represents the power of white Gaussian noise, which is spectrally flat. Therefore, a sloped line is a salient feature of intermodulation interference in an OFDM-based system; it necessary to detect the presence of intermodulation interference due to an offender, but it is not sufficient. However, since wireless spectrum is often distinctly associated with a wireless operator, we discount the possibility of a spurious spectrally sloped in-band transmission, making this condition *practically* sufficient to detect the presence of intermodulation interference.

Implementation dependent, the control-plane PRBs can have *equal* power levels on both sides of the spectrum—unlike the user-plane PRBs. This is because the control plane bandwidth is allocated per UE as one PRB on each side of the channel [10], providing the UEs with robustness against frequency-selective fading.

## IV. INTERMODULATION INTERFERENCE DETECTION

### A. Current methods of detection

**Introduction of test tones:** International standards for PIM testing [11], [12] specify two continuous wave tones to be injected at a fixed transmit power in the BS feeders to the antennas while the third-order intermodulation product (IM3) is monitored over a high-sensitivity receiver (e.g., with a spectrum analyzer). If IM3 products are observed (e.g., Fig. 2), then intermodulation interference is deemed detected in this BS. This approach has limitations: 1) it cannot be carried out in real time and 2) it would require the disconnection of the BS, hence the disruption of service for during the testing.

---

### Algorithm 1: Intermodulation Interference Detection

---

**Input:** RIP data  $\mathbf{R} \in \mathbb{R}^{|\mathcal{T}| \times N_{\text{PRB}}^{(u)}}$  for a BS with  $N_{\text{PRB}}$  PRBs.  
**Output:** Whether intermodulation interference is detected in the BS for the time of interest  $t \in \mathcal{T}$

- 1 Let  $\mathcal{P}^{(u)} := \{\text{PRB}_i : N_{\text{PRB}}^{(c)}/2 \leq i \leq N_{\text{PRB}} - N_{\text{PRB}}^{(c)}/2 - 1\}$
- 2 Initialize  $N_{\text{IM},t} := \text{False}$
- 3  $\mathbf{r} := [\mathbf{R}]_{t, \mathcal{P}^{(u)}}$
- 4  $(R^2, \beta_1) := \text{LinearRegression}(\mathcal{P}^{(u)}, \mathbf{r}_t)$
- 5 **if**  $(R^2 > \epsilon_{\text{linear}})$  **and**  $(|\beta_1| > \epsilon_{\text{slope}})$  **then**
- 6 |  $N_{\text{IM},t} := \text{True}$
- 7 **end**
- 8 **return**  $N_{\text{IM},t}$

---

**OFDM channel noise generator:** The OFDM channel noise generator (OCNG) is specified in the industry standards for 5G [4]. It introduces channel noise as simulated load on the downlink frequency bands for both FDD and TDD. Once enabled, the RTP of uplink frequency bands is monitored for an anomaly (e.g., abrupt rise) at the time the OCNG was activated. Anomaly that follows the OCNG activation/deactivation patterns means that intermodulation interference is detected. Testing with OCNG often requires loading the BS to the maximum (i.e., on all PRBs), which would generate interference and impact the channel quality and capacity on the PRBs belonging to the neighboring BSs.

### B. Proposed

Let  $\mathbf{R}$  be the user-plane RIPs measurements of a given BS collected periodically and sorted column-wise per PRB. Thus,  $\mathbf{R} \in \mathbb{R}^{|\mathcal{T}| \times N_{\text{PRB}}^{(u)}}$ , where  $\mathcal{T}$  is the set of measurements collection time window at a given periodicity (e.g., hourly) [3].

Let us formulate our proposed method as a detection problem. Thus, a binary hypothesis testing is formulated where for a given BS, the null hypothesis  $\mathcal{H}_0$  denotes absence of intermodulation interference while the alternative hypothesis  $\mathcal{H}_1$  denotes the presence of intermodulation interference. These instances of absence or presence are studied through the use of linear regression, which allows us to study if the RIP slopes with the PRBs. We choose linear regression to avoid having to deal with training and test data. Then, depending on the slope value  $\beta_1$  and the score of fit ( $R^2$ ) there are the following qualitative cases: 1) poor line fitting, 2) good line fitting and a small slope, and 3) good line fitting and a large slope. It should be clear that case 3 represents  $\mathcal{H}_1$ .

**Poor line fitting:** With  $R^2 < \epsilon_{\text{linear}}$ , the relationship between RIP and the PRBs is not linear enough to conclude the existence of intermodulation interference on the BS. For example, there could be either 1) narrow-band interferers that impact only a select group of PRBs (which have low score of fit) or 2) peaks due to spectral leakage are in the receive band.

**Good line fitting:** With  $R^2 \geq \epsilon_{\text{linear}}$ , the relationship between RIP and the PRBs has enough linearity where the slope  $\beta_1$  is meaningful. In this case there are two potential outcomes: 1)  $|\beta_1| < \epsilon_{\text{slope}}$  which means that the slope is too low and therefore no intermodulation interference exists or 2)

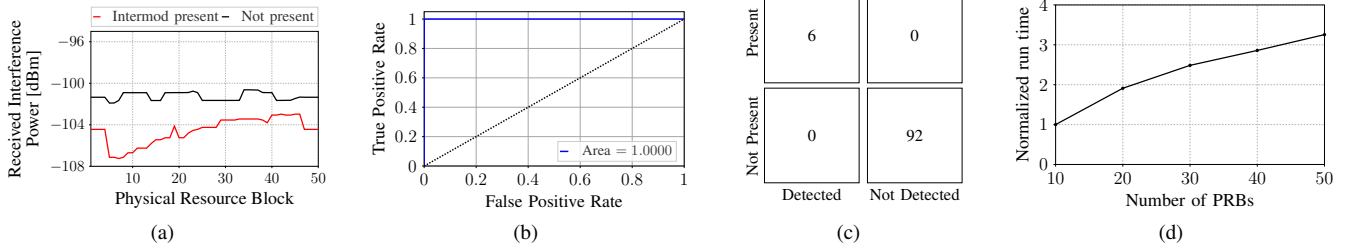


Fig. 5. Simulation results: (a) RIP vs PRB for two cases: intermodulation interference is present and is not present (b) receiver operating characteristic plot (c) confusion matrix and (d) normalized run time vs number of PRBs.

$|\beta_1| \geq \epsilon_{\text{slope}}$  and therefore intermodulation interference exists. In perspective,  $R^2 = 0.81$  in the fitted regression line in Fig. 3b.

**Algorithm outline:** In Algorithm 1, a row vector  $\mathbf{r}$  from the matrix  $\mathbf{R}$  is linearly regressed against the user-plane PRBs. For example, in a BS with  $N_{\text{PRB}}^{(u)} = 42$ , an hourly measurement for this BS would be a row vector with 42 entries. The regression is used to suggest if intermodulation was detected for this measurement. This is repeated for all measurements in  $\mathcal{T}$ .

**Parameter tuning:** The choice of  $\epsilon_{\text{linear}}$  and  $\epsilon_{\text{slope}}$  define the threshold at which we reject the null or alternative hypothesis. In order to find detection optimal values of these parameters, a receiver operating characteristic (ROC) curve is constructed based on a grid search over the space values that these parameters can assume. We select the values that correspond to the highest area under the ROC curve. This effectively minimizes the errors of rejecting  $\mathcal{H}_0$  when it is true (i.e., no intermodulation interference is present) and also minimizes the error of not rejecting  $\mathcal{H}_0$  when it is false (i.e., intermodulation interference is likely present). These are known as Type I and Type II errors, respectively.

**Run-time complexity:** The run-time of the proposed algorithm for one BS given the two learning features is linear in the number of PRBs in that BS, as we show in Section V.

**Benefits:** Unlike the current methods, our proposed algorithm does not have limitations with respect to implementation time or impacting users in the service area of the serving BS or any of the neighboring BSs. Furthermore, due to its constant run-time complexity, it can be run in real-time.

## V. SIMULATION

### A. Setup

We use a mobile operator dataset comprising two tables: 1) hourly RIP and RTP per receive branch 2) binary labels denoting whether intermodulation interference is detected through OCNB. This dataset has 100 rows representing measurement records of different BSs collected at different hours and days. Each BS has at least two frequency bands, each of  $B = 10$  MHz and has  $N_{\text{SC}} = 12$ ,  $N_{\text{PRB}} = 50$ , and  $N_{\text{PRB}}^{(u)} = 42$ . We drop any measurement record with an average RTP below  $N_0 + 10 \log B = -104$  dBm since these are unlikely to have experienced interference. To find the detection performance optimal value  $\epsilon_{\text{linear}}^*$ , we choose from a set of values that correspond to strong linear correlation  $\{0.95, 0.9, 0.85, 0.8\}$ .

Similarly, for  $\epsilon_{\text{slope}}^*$ , we choose from a set of values that correspond to high RTP  $\{1.03, 1.05, 1.07, 1.09, 1.11\}$ . We normalize the linear regression features and enable the intercept.

### B. Discussion

We start the discussion examining Fig. 5a. This figure shows two RIP vs PRB plots. The sloped line is suggestive of the presence of intermodulation, as motivated earlier. The patterns superimposed on the lines are due to uplink PRB allocation (e.g., due to traffic) or other types of impairments.

Next, we ask the following two questions: 1) how well does the proposed intermodulation interference detection algorithm perform in a realistic network? and 2) what is the impact of the number of PRBs on the run-time of the proposed algorithm?

To answer the first question, we compare the performance of our proposed algorithm against the labels. The ROC curve in Fig. 5b shows perfect prediction compared to the OCNB detection method which means that the algorithm always rejects the false hypothesis and thus detects intermodulation when it is present. This shows that testing for a sloped line in the interference pattern (using linear regression) is sufficient for intermodulation interference detection purposes. In perspective, there are 98 records in the data (out of 100) the average RTP of which is greater than  $-104$  dBm. Out of these, 6 belong to BSs that have intermodulation interference while 92 do not. Our proposed algorithm correctly detects whether a measurement record represents intermodulation interference as shown in the confusion matrix in Fig. 5c.

Finally, answering the second question, Fig. 5d shows that the proposed algorithm runs in  $\mathcal{O}(N)$ , where  $N := |\mathcal{P}|$ , making it suitable for advanced radio resource management procedures such as carrier aggregation.

A follow-up question stemming from this discussion is: if the receive band were wide enough to cover not only the linear region due to spectral leakage, but also the main peak, or if other narrow-band interferers existed along the intermodulation. In such a case, how would the detection algorithm perform? The answer is this would no longer be a linear characteristic and the  $R^2$  value of linear regression is likely to correspond to weak linear correlation. Other supervised machine learning algorithms would then need to be used to account for the evident non-linearity, which may also have a non-linear run-time complexity.

## VI. CONCLUSION

In this paper, we proposed a novel method to detect the presence of intermodulation interference in an OFDM-based system without the need of test tones or noise simulators as specified in industry standards. We showed salient intermodulation spectral characteristics that are due to FFT. This method uses machine learning in the form of linear regression of the received interference power as a function of the PRBs. Based on this method, we constructed an algorithm that detects intermodulation interference in linear run time making it suitable for real-time radio resource management applications in O-RAN, B5G, or 6G. An interesting extension is when the receive frequency band experiences nonlinearities due to either spectral leakage or other narrow-band interferers.

## REFERENCES

- [1] O-RAN Alliance. O-RAN: Towards an Open and Smart RAN. 2018. [Online]. Available: <https://www.o-ran.org/resources>
- [2] B. Jang, H. Kim, Y. Seo, S. Im, and S. Hong, "Mitigation of the third-order passive intermodulation distortion interference on uplink signal," in *Intl. Conf. on Elect., Infor., and Commun.*, Jan. 2019, pp. 1–3.
- [3] F. B. Mismar and J. Hoydis, "Unsupervised learning in next-generation networks: Real-time performance self-diagnosis," *IEEE Communications Letters*, vol. 25, no. 10, pp. 3330–3334, Oct. 2021.
- [4] 3GPP, "NR; User Equipment radio transmission and reception," 3rd Generation Partnership Project, TS 38.101, Oct. 2018.
- [5] 3GPP, "NR; NR and NG-RAN Overall Description," 3rd Generation Partnership Project, TS 38.300, Jul. 2020.
- [6] L. Martínez Marrero, L. Sadamori, S. Dominiak, U. Dersch, and J. T. Gómez, "Improving Soft Decoding by Spectral Leakage Reduction in Presence of Narrow Band Interference in PLC," *IEEE Access*, vol. 7, pp. 79 491–79 502, 2019.
- [7] F. B. Mismar and B. L. Evans, "Deep learning in downlink coordinated multipoint in new radio heterogeneous networks," *IEEE Wireless Communications Letters*, vol. 8, no. 4, pp. 1040–1043, Aug. 2019.
- [8] 3GPP, "LTE; Evolved Universal Terrestrial Radio Access; Physical layer; Measurements," 3rd Gene. Part. Proj., TS 36.214, Jul. 2018.
- [9] M. Cerna and A. F. Harvey, "The Fundamentals of FFT-Based Signal Analysis and Measurement," NI, Jul. 2000.
- [10] 3GPP, "LTE; Evolved Universal Terrestrial Radio Access; Physical channels and modulation," 3rd Gene. Part. Proj., TS 36.211, Apr. 2017.
- [11] International Electrotechnical Commission, "Passive RF and microwave devices, intermodulation level measurement - Part 1: General requirements and measuring methods," IEC, May 2012.
- [12] 3GPP, "Passive Intermodulation (PIM) handling for Base Stations (BS)," 3rd Generation Partnership Project, TR 37.808, Sep. 2013.